

Graphitic-Carbon Nitride Embedded PVDF-HFP Film for Enhanced Performance of Piezoelectric Nanogenerator

A DISSERTATION REPORT

**SUBMITTED IN PARTIAL FULFILLMENT OF THE REQUIREMENTS
FOR THE AWARD OF THE DEGREE
OF**

**MASTERS OF SCIENCE
IN
PHYSICS**

Submitted by:
SHIVENDER SINGH BHANDARI
2K23/MSCPHY/58
&
ADITYA ANAND
2K23/MSCPHY/04

Under the supervision of
DR. BHARTI SINGH



DEPARTMENT OF APPLIED PHYSICS

DELHI TECHNOLOGICAL UNIVERSITY

(Formerly Delhi College of Engineering)

Bawana Road, Delhi – 110042

JUNE, 2025

DECLARATION

We hereby certify that the work which is presented in the Major Project-II/Research Work entitled "**Graphitic-Carbon Nitride Embedded PVDF-HFP Film for Enhanced Performance of Piezoelectric Nanogenerator**" in fulfilment of the requirement for the award of the Degree of Bachelor/Master of Technology in Department of Applied Physics, Delhi Technological University, Delhi is an authentic record of my/our own. carried out during a period from June 24 to June 25, under the supervision of **Dr. Bharti Singh**.

The matter presented in this report/thesis has not been submitted by us for the award of any other degree of this or any other Institute/University. The work has been communicated in Scopus indexed journal with the following details.

Title of the Paper: Graphitic-Carbon Nitride Embedded PVDF-HFP Nanocomposite Film for Improved Performance of Piezoelectric Nanogenerator.

Authors names: Shivender Singh Bhandari, Aditya Anand, Shilpa Rana, Dibyajyoti Giri, Jasvir Dalal, Bharti Singh

Name of journal: Discover Materials

Status of paper : communicated

Date of paper communication : 26 May, 2025

Date of paper publication : Yet to be published.



Shivender Singh Bhandari

23/MSCPHY/58



Aditya Anand

23/MSCPHY/04

SUPERVISOR CERTIFICATE

To the best of my knowledge, the above work has not been submitted in part or full for any Degree or diploma to this University or elsewhere. I, further certify that the publication and indexing information given by the students is correct.



Place: Delhi

Dr. Bharti Singh

Date: 09/06/2025

ACKNOWLEDGEMENT

We would like to express our deepest sincere gratitude to our supervisor, Dr. Bharti Singh, Assistant Professor, Department of Applied Physics, Delhi Technological University for giving us the opportunity to work under her guidance and for constant inspiration and incessant support throughout the project. We take this opportunity to express our indebtedness to our supervisor for her enthusiastic help, her expertise, brilliant ideas, valuable suggestions, and constant encouragement. We are grateful to acknowledge the constant help and convenience at every step of our project by all the lab members (Ph.D. scholars), Dept. of Applied Physics. Lately, we are thankful to our families and friends for their love, care, and support who patiently extended all sorts of help for accomplishing this task.

ABSTRACT

Piezoelectric nanogenerators (PENGs) have gained attention as sustainable energy harvesters for wearable electronics and IoT systems by converting ambient mechanical energy into electricity. This study demonstrates a high-performance flexible PENG based on poly(vinylidene fluoride-co-hexafluoropropylene) (PVDF-HFP) nanocomposite films loaded with graphitic carbon nitride (g-C₃N₄) nanofillers at varying concentrations (0, 1, 3, and 5 wt%). Structural analyses via X-ray diffraction (XRD), Fourier-transform infrared spectroscopy (FTIR), and scanning electron microscopy (SEM) validated the homogeneous dispersion of g-C₃N₄ within the polymer matrix and its role in enhancing the electroactive β -phase content. When subjected to mechanical excitation via electrodynamic shaker testing, the 5 wt% g-C₃N₄/PVDF-HFP composite achieved optimal electrical outputs, generating an open-circuit voltage of 21.2 V and a short-circuit current of 14.24 μ A—a marked improvement over pristine PVDF-HFP films. The performance enhancement correlates with the filler-induced polarization and crystalline phase modification in the polymer. These findings underscore the viability of g-C₃N₄-reinforced PVDF-HFP nanocomposites as efficient, flexible energy harvesters for self-powered wearable technologies.

CONTENT

CHAPTER-1

10-25

INTRODUCTION AND OBJECTIVES

1.1 INTRODUCTION

1.1.1 OBJECTIVES

1.2 LITERATURE REVIEW

1.2.1 Nanoparticles and Nanotechnology

1.2.2 Nanoparticle Synthesis Techniques

1.2.2.1 One-Step Pyrolysis Process

1.2.2.2 Hydrothermal Synthesis

1.2.2.3 Sol-Gel

1.2.3 PVDF and its copolymer

1.2.4 2D Materials

1.2.5 Graphitic carbon Nitride (g-C₃N₄) nanosheets

1.2.6 ENERGY HARVESTING

1.2.6.1 Nanogenerators

1.2.6.1.1 Piezoelectric Nanogenerators (PENGs)

1.2.6.1.2 Triboelectric nanogenerators (TENGs)

1.2.6.1.3 Material selection for Nanogenerators

CHAPTER 2

26-28

MATERIALS AND METHODS

2.1 CHEMICALS

2.2 SYNTHESIS METHODS

2.2.1 Synthesis of Graphitic Carbon Nitride (g-C₃N₄) powder

2.2.2 Synthesis of PVDF- HFP/g-C₃N₄ films

CHAPTER 3

29-40

CHARACTERISATION, RESULTS AND DISCUSSIONS

3.1 CHARACTERIZATION TECHNIQUES

3.2 RESULTS

3.2.1 XRD analysis of Graphitic Carbon Nitride (g-C₃N₄)

3.2.2 Field Scanning Electron Microscopy (SEM)

3.2.3 XRD analysis of PVDF-HFP/ g-C₃N₄ nanocomposite film

3.2.4 FTIR analysis of thin films

3.2.5 Polarisation-Electric field(P-E) curve

3.2.6 Electrical Measurements

3.2.7 Application of Piezoelectric Nanogenerator

CHAPTER 4

41-42

CONCLUSIONS AND FUTURE SCOPE

4.1 CONCLUSIONS

4.2 FUTURE SCOPE

LIST OF FIGURES

Figure 1.1. Different types of nanoparticle synthesis techniques.

Figure 1.2: Structure of graphitic carbon nitride nanoparticle.

Fig. 1.3 Steps of Working mechanism of Piezoelectric Nanogenerator

Fig. 1.4 Different types of working modes of Triboelectric Nanogenerators

Fig. 1.5 Triboelectric series on the basis of their electroactivity

Figure 2.1: Synthesis of Graphitic Carbon Nitride (g-C₃N₄) powder.

Figure 2.2: Synthesis of PVDF-HFP/ g-C₃N₄ thin films.

Figure 3.1. XRD Plot of Graphitic Carbon Nitride (g-C₃N₄) powder.

Fig.3.2 FESEM image of the graphitic carbon nitride nanofilm.

Fig. 3.3 presents the XRD spectra of pristine PVDF-HFP(PHG0) and g-C₃N₄ incorporated PVDF-HFP films (PHG1, PHG3, PHG5).

Figure 3.4. FTIR spectra of PVDF-HFP/ g-C₃N₄ thin film with different wt. % of g-C₃N₄.

Fig.3.5 PE loop for the fabricated thin films.

Fig. 3.6 Open-circuit voltage for (a)PVDF-HFP (b) PVDF-HFP with 1 wt% g- C₃N₄ (c) PVDF-HFP with 3 wt% g- C₃N₄ (d) PVDF-HFP with 5 wt% g- C₃ N₄.

Fig.3.7 Short-circuit current for (a)PVDF-HFP (b)PVDF-HFP with 1 wt% g- C₃N₄ (c) PVDF-HFP with 3 wt% g- C₃N₄ (d) PVDF-HFP with 5 wt% g- C₃N₄.

Fig. 3.8 Working Mechanism of Piezoelectric Nanogenerator

Fig. 3.9 Open-circuit voltage for PENG under the application of the force from the (a) finger (b) thumb, (c) Schematic circuit diagram for application of PENG in lighting up an LED, and (d) LED lit up by PENG

LIST OF TABLES

Table 1: For the same amount of PVDF-HFP the variation in the wt% of g-C₃N₄.

Table 2: β -Phase of g-C₃N₄ incorporated PVDF-HFP film with different wt %.

Table.3 Comparison of PENG performance as a function of nanofiller concentration

CHAPTER 1

INTRODUCTION AND OBJECTIVES

1.1 INTRODUCTION

Advancement in technology demands for introduction of sustainable and efficient energy sources for the human consumption. This will not just reduce the dependence on the insufficient fossil fuels but will also solve the environmental crisis. The advancement in the integrated circuits in the recent times have shown the miniaturization of electronic devices which are becoming more portable, wearable and even used as implants. The dependence of electronic devices on batteries is a well known fact and the life of these batteries is believed to be very short for consumption. This limits the use of batteries in long term use of electronic devices prone to the device to frequent replacement of these energy sources, i.e. batteries. Furthermore, the byproduct of these batteries' consumption has resulted in widespread environmental contamination. Portable energy storage technologies are the most well-known substitute for these sources. There was growing desire for sustainable, maintenance-free power options that would lessen reliance on traditional batteries. Energy collection from a variety of sustainable sources was investigated in order to meet these demands. Among these, mechanical energy is the best source for energy harvesting because of its accessibility. In 2006, this prompted researchers to develop a novel energy harvesting device called nanogenerators. But, these nanogenerators were initially were temperature, and catalyst dependent which made them less of preference to be utilised further for future use. Since their creation, piezoelectric nanogenerators have garnered a lot of interest due to their ability to use piezoelectric nanomaterials to transform minute amounts of ambient irregular kinetic energy into electrical power. Real-time LED illumination is one of the PENGs' real-time applications. The main

emphasis was put on the enhancement of the output performance of the PENG which was done by works done on material selection, innovative device design and structural integration. On the other hand the other type of nanogenerator which is the triboelectric nanogenerator (TENG) which harnesses ambient mechanical motions as the source to generate electrical energy. The TENG has a number of benefits over other energy harvesting technologies, including cost effectiveness, light weight, and high power density, which contribute to the desired output. It operates on the principles of triboelectrification and electrostatic induction. It has mainly four modes of operation including contact separation mode, lateral sliding mode, single electrode mode and free-standing triboelectric layer mode.[1]

In around 50 years, nanotechnology has grown to become the foundation for incredible industrial applications and exponential growth [2]. Because of their special structure, nanoparticles can have remarkably large surface areas. Nanostructures are very different from their bulk counterparts in these aspects, and can exhibit exceptional optical, mechanical, electrical, catalytic, and magnetic properties. The properties of nanomaterials can be precisely tailored to meet particular needs by carefully controlling their size, shape, synthesis conditions, and appropriate functionalization [3].

1.1.1 OBJECTIVES

- To synthesise Graphitic Carbon Nitride Powder using One step Pyrolysis method.
- To optimize the nanofiller concentration of the polymer matrix.
- Fabrication of the nanofilms with graphitic carbon nitride as the nanofiller with varying weight percentage.
- Fabrication of the Piezo-nanogenerator (PENG).
- Measurement of the output performance of PENG.
- Utilization of the piezoelectric nanogenerator as an electronic device power source.
- Discussion of future aspects of the application of PENG.

1.2 LITERATURE REVIEW

1.2.1 Nanotechnology and Nanoparticles

In physical, chemical, and biological domains, nanotechnology encompasses the creation of nanostructures, the use of nanocomposites, and the utilization of all experimental techniques at atomic to submicron sizes. Examined here is a wide range of engineering physics, fabric technology, and manufacturing. Similar to the effects of mobile and molecular biology, semiconducting material technology, and statistical technology in the previous century, it has an influence on our environment and economy in the present days. Our lives have advanced in every way due to nanotechnology, which has transformed the way commercial issues in areas such as feasible materials, nanocomposite manufacturing, electronics devices, medicine supply, electricity and water, biotech, record-keeping methods, and national security have been handled. Nanotechnology is a modern industrial revolution that will have a huge influence on our economy and society[4]. Therefore, the creation of 2D materials is a topic that scientists and researchers are more interested in exploring.

1.2.2 Nanoparticle Synthesis Techniques

Nanoparticles can be synthesized by different techniques. These methods can be used to create dry particles as well as nanoparticles, which can be distributed in a liquid or gaseous media. Nanostructures can be produced by beginning with atoms or by shrinking microparticles to nanoparticle size[5].

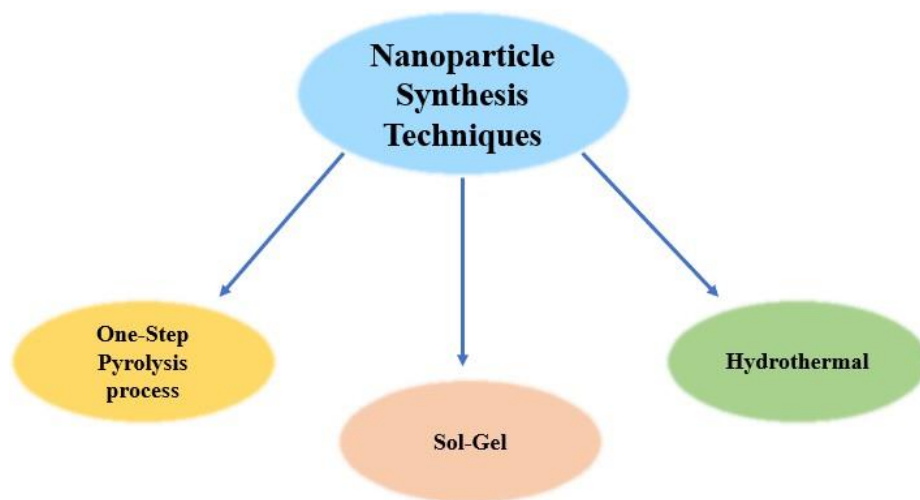


Figure 1.1: Different types of Nanoparticle synthesis techniques.

1.2.2.1 One-Step Pyrolysis Process.

One step pyrolysis is a thermal decomposition method conducted in an inert environment, commonly used for the synthesis of nanomaterials. In this technique, a precursor material is subjected to high temperatures to decompose into smaller, stable nanostructures. The process is straightforward and it is also one of the processes which is less complex and less time consuming for material synthesis. The precursor such as urea is placed in the muffle furnace at $600^{\circ}\text{C} - 700^{\circ}\text{C}$ for around 3hrs and then the sample is cooled and a powder form of the nanomaterial is obtained in the process.

The readily available precursors makes process economically viable, also the parameters like temperature, heating rate and precursor concentration can be tuned to achieve desired sizes and shapes of the material which is very important aspect keeping in mind the importance of particle size in the nanomaterial synthesis. It is a highly efficient and versatile technique for nanomaterial synthesis. Although it causes high energy costs and precision control but these factors can be optimized going forward.

1.2.2.2 Hydrothermal Synthesis

The hydrothermal method is widely used to produce solids such as fluorides, ceramics, complex oxides, microporous crystals, and superionic conducting materials. Magnetic materials and luminescence phosphors are also produced with the help of it. Novel condensed materials, such as stacking sequence material, are also accessible through it. Additionally, the synthesis of thin films, helical and chiral structures, and nanoscale particles is made possible.

"Hydrothermal synthesis" refers to the method of generating compounds by chemical reactions in a heated, sealed solution that is heated above ambient temperature and pressure[6].

1.2.2.3 Sol-Gel

One method used to create solid materials using tiny molecules is the sol-gel process. The sol (or solution) changes during this chemical process, becoming a biphasic system that resembles a gel. There are two phases to this system: a liquid phase and a solid phase. The liquid phase can have various morphologies, such as single particles or networks of linked polymers. Finely ground and homogenous ceramic powders can be produced via precipitation. These single- and multi-component powders at the nanoscale are produced for use in dentistry and biomedicine[7].

1.2.3 Polyvinylidene Fluoride (PVDF) and its copolymer

Triboelectric polymers have recently attracted a lot of interest. These include polyvinylidene fluoride (PVDF) and its copolymers, hexafluoropropylene (HFP), tri-fluoroethylene (TrFE), bromotrifluoroethylene (BTFE), and chlorotrifluoroethylene (CTFE). TrFE has received the most attention out of all of these[24]. The property of PVDF-HFP of being more stable and highly flexible is found to be very promising for its use as negative tribo-electric layer in TENG fabrication. The property of the PVDF-HFP to show high β phase content can be utilised. There are three phases in the PVDF-HFP material: α , β , and γ phases. Among these the β phase exhibits the highest piezoelectric coefficient, which makes it suitable to be used in PENG[8].

α , β , γ , and δ are the four distinct crystalline phases of PVDF-HFP polymer. Pressure, heat, and an electrical field can all be used to interconvert these phases. Although the β and γ phases are polar phases, the α -phase is the most stable and non-polar phase in thermodynamics. Polar PVDF is used to collect energy in electronics, sensors, actuators, and other devices.. The β phase is the most significant of all the crystalline phases because of its increased polarization and piezoelectric sensitivity[9]. Owing to this characteristic, several attempts have been undertaken to improve the β phase of PVDF-HFP's thermal, mechanical, and chemical characteristics[10]. PVDF-HFP has strong film-forming qualities that make it equivalent to applications for nanogenerators. Nevertheless, pure PVDF-HFP produces very little electrical energy in real-world applications. They so require certain procedures like poling and the addition of filler materials, among others. The primary reasons we think about introducing nanofiller materials are their many benefits, which include reduced costs, easier production, and higher electrical output. A number of widely used nanofillers, such as ZnO and its different nanostructures, graphitic carbon nitride, reduced graphene oxide, SnSSe, are utilized to modify the symmetry of PVDF-HFP and enhance its triboelectric properties[11, 12].

1.2.4 2D Materials

Two-dimensional (2D) layered non-centrosymmetric materials have enormous promise for electronic devices and nanoscale electromechanical systems. Since the discovery of graphene in 2004, atomically thin 2D substances have attracted a lot of attention recently due to their extraordinary and distinctive mechanical, optical, magnetic, and electric properties[18]. In recent years, with great advances in synthesis techniques, more and more 2D materials beyond graphene have been successfully produced. Among these, graphitic carbon nitride (g-C₃N₄) has drawn a lot of interest. Because of their special properties, such as flexibility, transparency, mechanical stability, and nontoxicity, two-dimensional materials are the greatest choices for building energy harvesters like TENGs[13].

Several intriguing characteristics of 2D materials include their high surface to volume ratio, stackable layers, ultra-thinness, transparency, and flexibility. There are several uses for 2D materials in the areas of energy generation, energy storage, optoelectronics, sensors, detectors, and electrochemical catalysis.

1.2.5 Graphitic Carbon Nitride Nanosheets

There is a class of polymeric materials, namely Carbon Nitrides which mainly consists of carbon and nitrogen. They are utilized in many different applications, such as fillers for nanoparticles in nanogenerators, and are mostly produced by carbon materials by substituting nitrogen for the carbon atom. The C-N bond assembly in g-C₃N₄ is devoid of electron localization in the π state. Graphitic Carbon Nitride is not only the most stable allotrope of carbon but also has enhanced surface properties which makes it suitable for application in the nanogenerators [14].

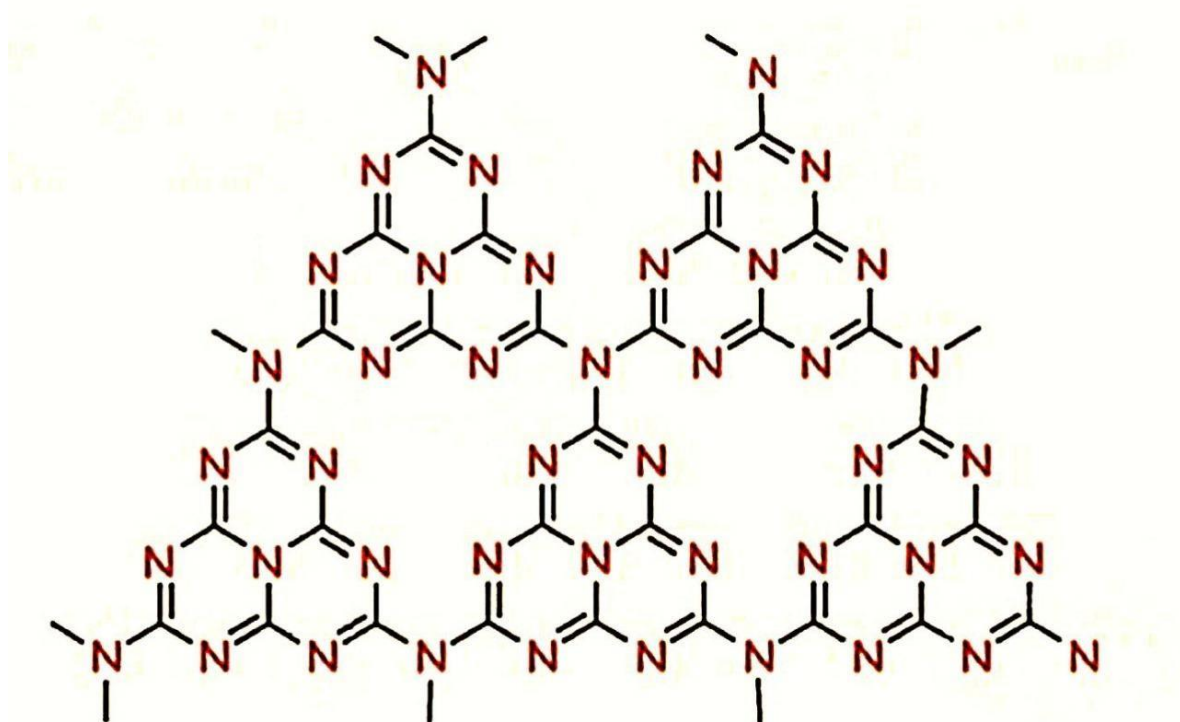


Figure 1.2 Structure of Graphitic Carbon Nitride.

1.2.6 Energy Harvesting

The limited supply of energy in today's world limits human and economic advancement. Investigating clean and sustainable energy sources should be one of the main approaches to this problem. Furthermore, carbon emissions from renewable energy sources, such as solar or mechanical power, do not contribute to global warming or environmental degradation and only very slightly do so. There's always more energy than we could ever need in the ecosystem, yet it gets “wasted”[15]. Due to their ability to transform mechanical energy from the environment into useable electrical energy, piezoelectric nanogenerators have garnered a lot of attention lately. So far, a variety of Triboelectric materials have been studied, such as g-C₃N₄, ZnO, PZT, etc[16].

1.2.6.1 Nanogenerators

In the last few decades the use of nanogenerators as a energy harvesting device has come into effect. These nanogenerators are mainly classified as piezoelectric nanogenerators (PENG) and triboelectric nanogenerator (TENG) which are used to harness ambient mechanical energy.

1.2.6.1.1 Piezoelectric Nanogenerators (PENGs)

The devices that use the piezoelectric effect to capture mechanical energy from the environment are called piezoelectric nanogenerators (PENG). The prepared PENG undergoes application of force on both sides to produce electrical output. The alternate cycles of compression and relaxation results in the polarization of dipoles in the prepared film of the nanogenerator, leading to charge build-up on both the electrodes, and when the forces is released there is movement of charge in the reverse direction, resulting in an alternating electric current.

The behaviour of the piezoelectric effect can be explained using the fundamental constitutive equation,

$$\sigma_p = C_{pq} \epsilon_q - e_{kp} E_k \quad (1)$$

$$D_i = e_{iq} \epsilon_q + \kappa_{ik} E_k$$

Equation (1) illustrates coupled relationships where mechanical deformation and electric field are closely interdependent. In this case, E_k stands for the electric field, D_i for the electric displacement vector, σ_p for the stress tensor, C_{pq} for the elastic modulus tensor, ϵ_q for the strain tensor, and κ_{ik} for the dielectric tensor.. To analyse the coupled system, Gao et al.

employed a perturbation expansion approach, which led to a new concept of remnant displacement D_{Ri} being proposed.

$$\rho^R = -\partial D_{Ri} / \partial x_i \quad (2)$$

$$\Sigma^R = n^i D_{Ri}$$

$$D_{Ri} = e_{ip} \varepsilon_p \quad (3)$$

The resulting body charge ρ^R and surface charge Σ^R in the piezoelectric structure are directly influenced by the strain ε_p generated through external mechanical force. From this understanding, the working mechanism of PENGs can be described as follows: The body charge that develops in the piezoelectric material will cause a voltage differential between the electrodes when an external force is applied. This voltage differential will then drive the flow of electrons, producing electrical output. When the strain is evenly distributed throughout the piezoelectric layer, only surface charges remain as a residual effect. In such cases, the PENG behaves similarly to a pre-charged capacitor.

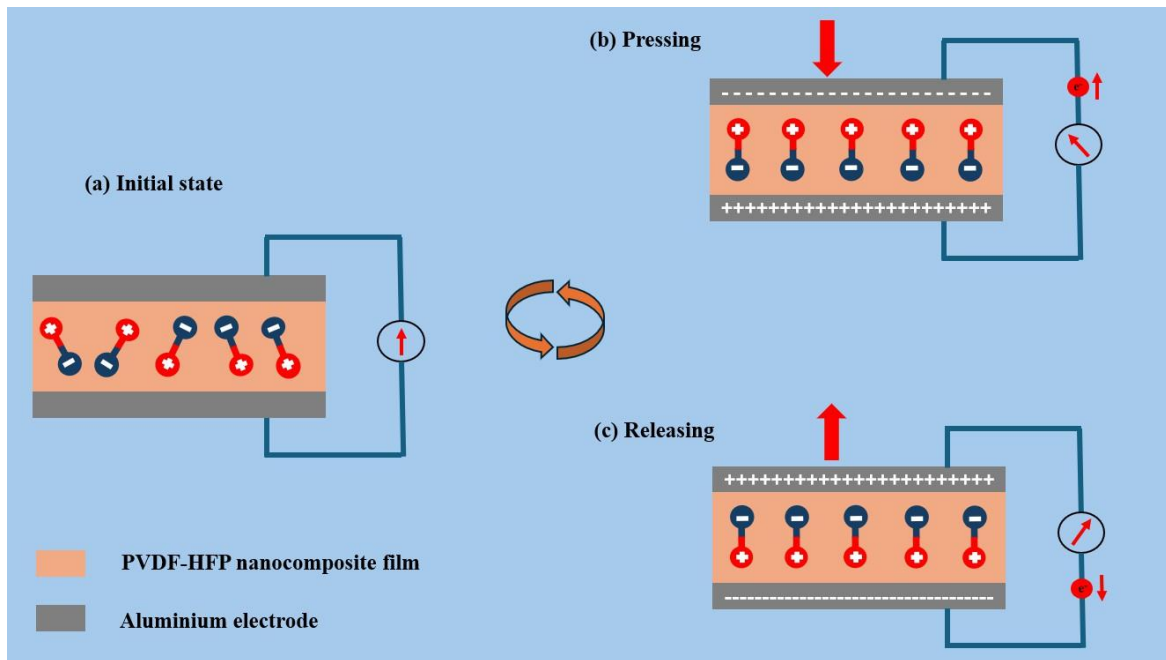


Fig. 1.3 Steps of Working mechanism of Piezoelectric Nanogenerator

1.2.6.1.2 Triboelectric Nanogenerators (TENGs)

The TENG primarily functions by linking the electrostatic induction and triboelectric effect. Triboelectric nanogenerators as a new energy technology has different applications like fundamental use as energy source in electronics devices. It features unparalleled advantages over other developed existing technologies, including high power density, light weight, small size, low cost, flexibility and even transparency [1]

Triboelectric effect occurs when a material becomes electrically charged when separated from an another material which the material was previously on contact with. Contact electrification and electrostatic induction are the two primary phenomena that are involved in the TENG's operational procedures. One phenomenon involving contact electrification is the upcoming. In contact of two materials or layers, whers either one material mechanically slides over the other or one material comes in contact with the other. This process leads to the accumulation of opposite charges on either layers.

Thus, the intrinsic characteristics of the material, such as the coefficient of friction, electron affinity, work function, and contact layers, are used in the contact electrification and have an impact on the electrical output of the TENG. Two tribo-materials with opposing electronegativities typically make up the TENG. Contact electrification causes an accumulation of equal and opposite charges on both surfaces when these layers come into contact. As the two layers separate further, electrostatic induction causes charges to be induced on the associated electrodes. An electron moves across the external circuit to neutralize the opposing charges on either electrode as a result of the potential difference created by the

buildup of charges on either side. The output of the contact separation cycle is an alternating current.

The TENG mainly operates in four modes:

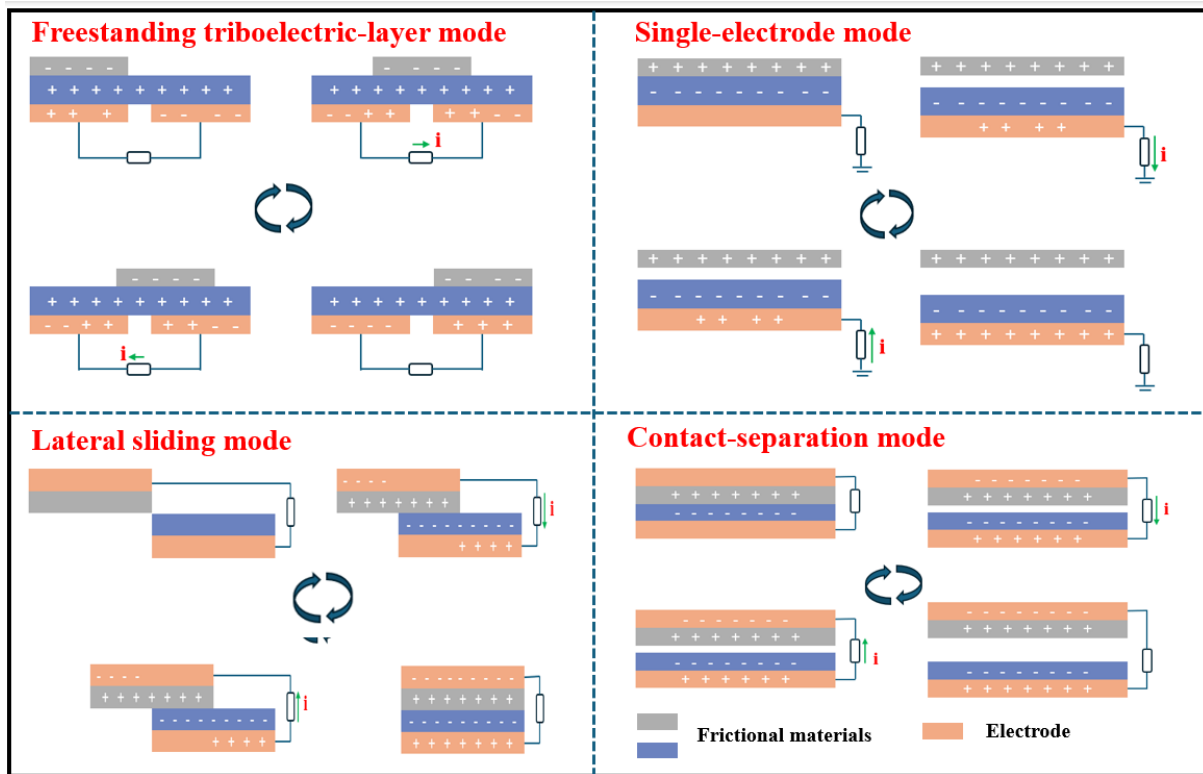


Fig. 1.4 Different types of working modes of Triboelectric Nanogenerators

1.2.6.1.3 Material selection for Nanogenerators

The material selection procedure of the PENGs are a multifaceted procedure requiring consideration of various factors which draws heavily from both, the intrinsic properties of the material and the specific requirements of the intended applications. The initiation of the selection procedure starts with the consideration of the piezoelectric materials available, which are broadly categorised into ceramics, single crystals, polymers, composites and nanostructured materials. Each of this category offers a wide variety of

advantages and limitations. Materials like lead zirconate titanate (PZT) and lead magnesium niobate-lead titanate (PMN-PT) exhibit high piezoelectric coefficients and energy conversion efficiency but are often brittle and may contain toxic elements such as lead, raising biomechanical and environmental concerns. In contrast, polymers like polyvinylidene fluoride (PVDF) are perfect for flexible and wearable devices because they are lightweight, flexible, and can be processed into a variety of shapes. Additionally, the selection process selects materials based on important piezoelectric properties, such as the piezoelectric charge constant (d), which indicates the material's capacity to produce electric charges under mechanical stress. The piezoelectric voltage constant(g), which relates to the voltage output, the electromechanically coupling factor(k), indicative of energy conversion efficiency, and the dielectric constant(ϵ), which influences impedance and voltage output. Mechanical properties such as the young's modulus are also considered to ensure compatibility with device substrates and to match the mechanical characteristics required by the application, whether it be for harvesting energy from vibration, pressure, or acoustic waves.

Additionally, scalability and processability are important parameters in material selection as the chosen material must be amenable to nano structuring techniques such as electrospinning, chemical vapor deposition, or solution processing, which essential for fabricating nanogenerators with high surface area and efficient energy conversion.

Material selection for the Triboelectric Nanogenerators is done on the basis of the triboelectric series, which is the series based on the polarities of frictional materials.

The basis for this series is these materials' capacity to acquire or lose electrons when in contact with other materials.

The materials at the top of the series have a greater affinity for positive charges because they are less electronegative (lower work function), while the materials at the bottom of the series (higher work function) will have a greater affinity for negative charges. For the material selection of different layers of TENG the use of the triboelectric series is done. The materials are selected on the basis of their difference in position in the triboelectric series as the further apart these materials will be from each other in the series the more compatible they are to be used as opposite layers in a TENG. More than fifty polymer materials' triboelectric series were recently quantified by Zou et al.

As part of a continuing expansion of this series, Dong et al. recently proposed metallic MXene as a trib-negative material with high conductivity and surface-terminated F atoms to independently acquire strong electro-negativity. The conductivity restrictions of the typical tribo-negative materials were overcome by MXenes.

Previously used materials for triboelectric layers were mostly polymers with well-known characteristics including friction coefficient, triboelectric surface charge density, and dielectric properties. But alternative 2D materials, such as graphitic carbon nitride (g-C₃N₄), can also be used to improve TENG performance.

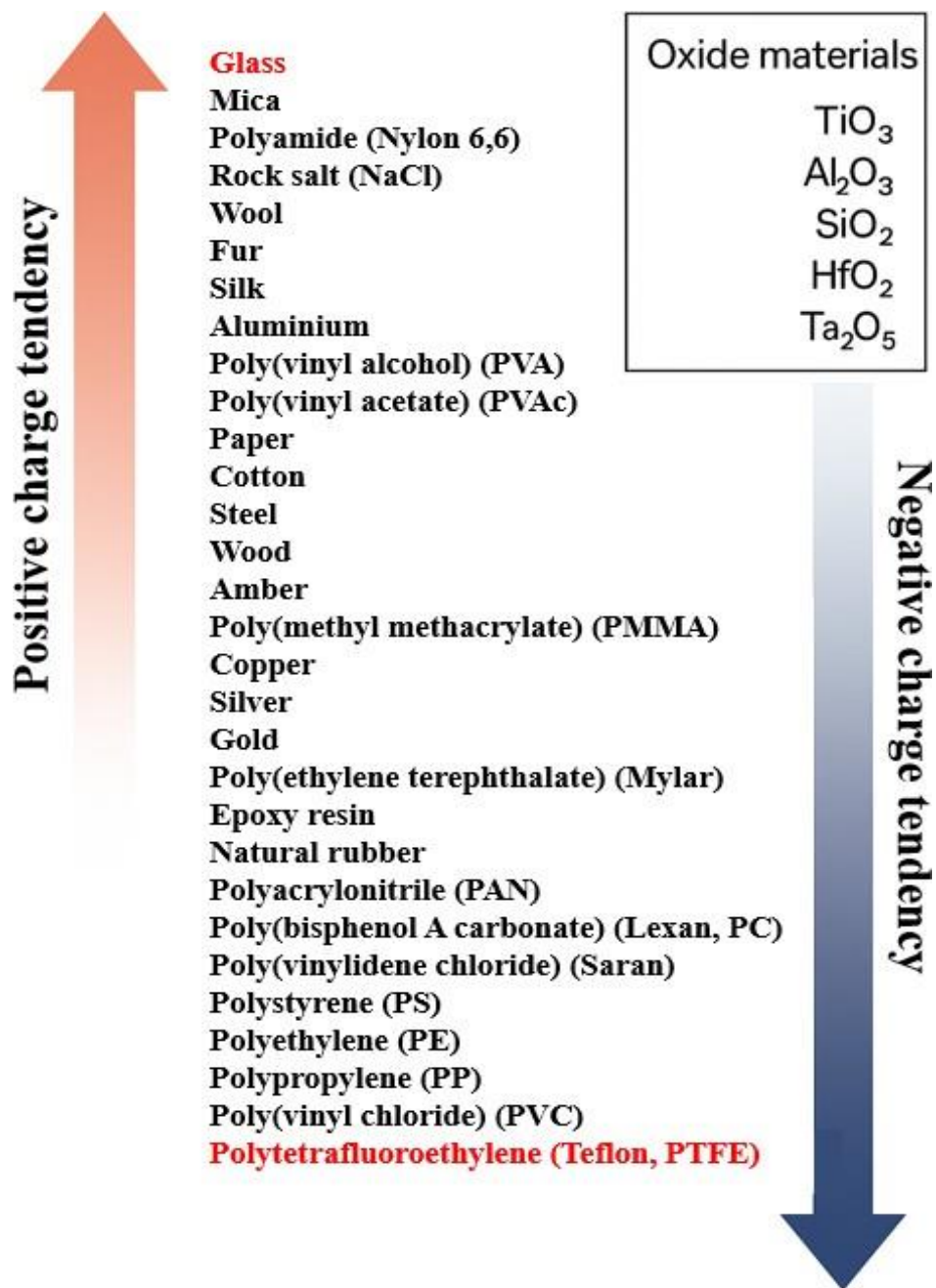


Fig. 1.5 Triboelectric series on the basis of their electroactivity

CHAPTER 2

MATERIALS AND METHODS

The synthesis of the Piezoelectric Nanogenerator was conducted after the synthesis of the constituents of the nanogenerators which included synthesis of graphitic carbon nitride nanofillers followed by the synthesis of the PVDF-HFP films with incorporation of the graphitic carbon nitride nanofiller with varying weight percentages.

2.1 Chemicals Used

Urea($\text{CH}_4\text{-N}_2\text{O}$), Polyvinylidene fluoride hexafluoropropylene (PVDF-HFP), Di-methyl fluoride(DMF), Ethanol, Acetone, Deionised water(DI water)

2.2 SYNTHESIS METHODS

2.2.1 Synthesis of g-C₃N₄ powder

The one-step pyrolysis method was used to create graphitic carbon nitride (g-C₃N₄). This approach used urea (CH₄-N₂O) as the precursor in its natural state without any pre- or post-treatment. A 50 milliliter crucible containing 10 grams of urea was covered with foil. The crucible was then put inside the muffle furnace, and the temperature within the furnace was raised steadily at a rate of 5 degrees Celsius per minute until it reached 650 degrees. For 180 minutes, this heating process was carried out. The furnace was shut off once the allotted time had passed, and the sample was allowed to cool to room temperature. On removal of the crucible from the furnace a powder sample was obtained. The powder sample was yellow in colour. The synthesis process is depicted in the Fig.2.1[17,18].

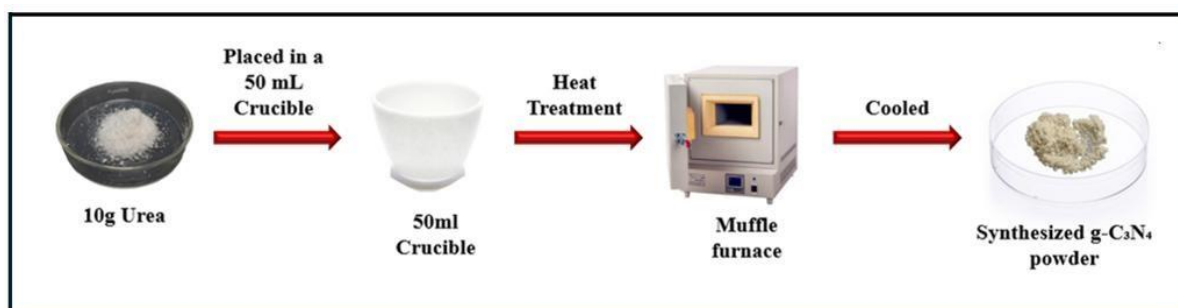


Figure 2.1: Synthesis of g-C₃N₄ powder

2.2.2 Synthesis of Polyvinylidene fluoride hexafluoropropylene (PVDF-HFP) films

In a beaker, 1g PVDF-HFP into 5ml DMF solution and then heat stirring the solution A for 120 minutes at 60 ° C . A solution B was prepared with different wt% of g-C₃N₄ was mixed in 5ml DMF solution and then ultrasonicated for 30 minutes .solution A and B are then mixed and stirred again for 60 minutes at 70 ° C. The films were formed from the prepared material using the drop casting method. These drop casted fil s were then placed in a vacuum over for 120 minutes. Because the thin films are hydrophobic, they were next submerged in DI-Water to separate them from the glass slide.

As illustrated in Fig. 2.2, we ultimately produce g-C₃N₄ PVDF-HFP flexible composite thin films with varying weight percentages (0%, 1%, 5%, and 7wt%) of g-C₃N₄, designated P0, P1, P3, P5, and P7, respectively.

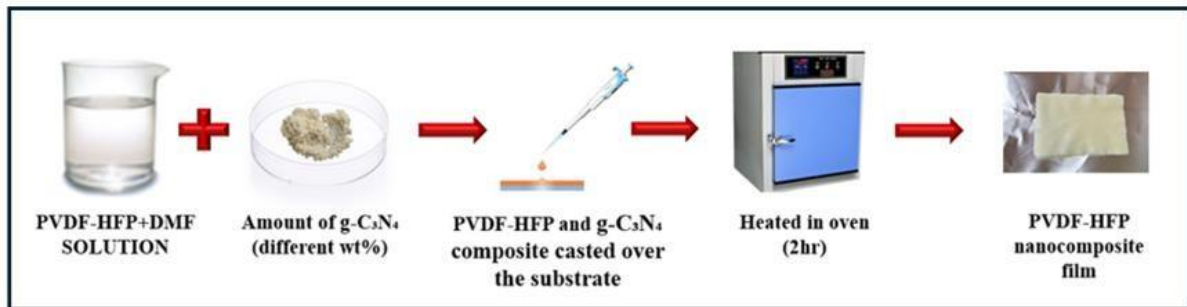


Figure 2.2: Synthesis of PVDF-HFP/ g-C₃N₄ thin films

PVDF-HFP (g)	DMF(ml)	Wt% of g-C ₃ N ₄	Quantity of g-C ₃ N ₄ (mg)
1	10	0	0
1	10	1	10
1	10	3	30
1	10	5	50

Table 1: For the same amount of PVDF-HFP the variation in the wt% of g-C₃N₄ .

CHAPTER 3

CHARACTERIZATION, RESULTS AND DISCUSSIONS

3.1 Characterization Techniques

The crystallinity and phase of the synthesized graphitic carbon nitride was done using the X-Ray diffractometer (XRD) (Cu X-ray source, 3KW) (JEOL Japan Model: JSM 6610LV). Using scanning electron microscopy (SEM), the synthesized graphitic carbon nitride sample's morphological and spectral characteristics were assessed. Characterization was done on the flexible g-C₃N₄-PVDF-HFP films and the heterostructure of the nanofillers with the PVDF-HFP matrix. through an X-ray source (X-Ray diffractometer, or XRD). Utilizing the Nicolet Is50 FTIR Tri- detector, a Fourier Transform Infrared spectroscopy (FTIR) spectrometer, the β -phase content of the manufactured thin film was examined in order to examine its morphological characteristics. The thin-film remanent polarization was investigated using the Polarization vs. Electric (P-E) field hysteresis plot. The digital multimeter (Keithley DMM6500) and digital storage oscilloscope (Tektronix, MD0500) were used for all electrical measurements following the manufacturing of the PENGs.

3.2 Results

3.2. XRD of Graphitic Carbon Nitride (g-C₃N₄)

The g-C₃N₄ powder's XRD pattern, displayed in Fig. 3.1, resembles the hexagonal phase of the typical JCPDS card No. 87-1526 [18]. The most prominent peak, which comes from the tri-s-triazine's in plane structural packing units, was observed at 27.37°, 13.01°, or the (002), (100) reflection plane.

The peak at 27.37° is caused by stacking of graphitic carbon nitride layers, while the peak at 13.01° is a reflection of the in-plane structural packing of the tri-s-triazine units. There are similarities between the design and the hexagonal phase described in the standard JCPDS card No. 87-1526.

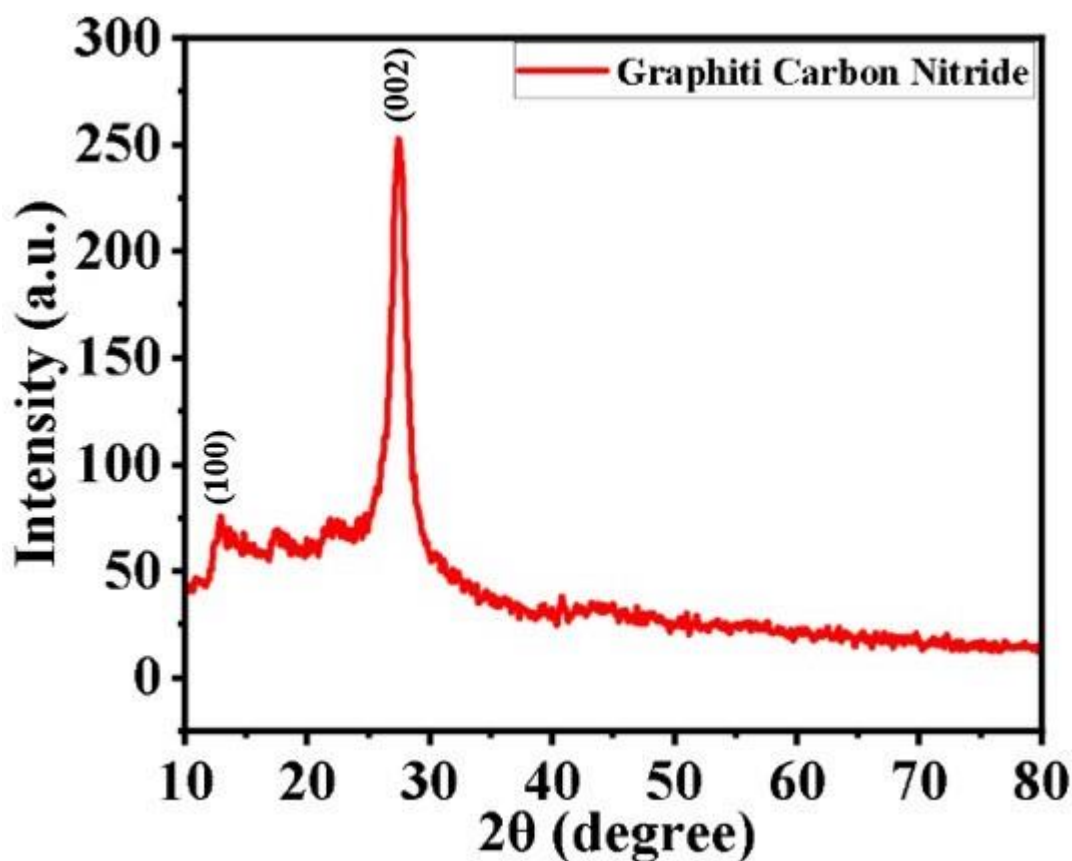


Figure 3.1. XRD Plot of g-C₃N₄ powder

3.2.2 Field Scanning Electron Microscopy (FESEM)

Field Scanning Electron Microscopy is used to examine the g-C₃N₄ morphology. The FESEM was carried out at 100nm magnification which helped in the analysis of the formation of the sheet like structure of the prepared sample of g-C₃N₄. The sample prepared at 550°C was

analysed and the sheet like morphology of the given sample as shown in the Fig.3.2 which confirms the successful synthesis of the nanosheets.

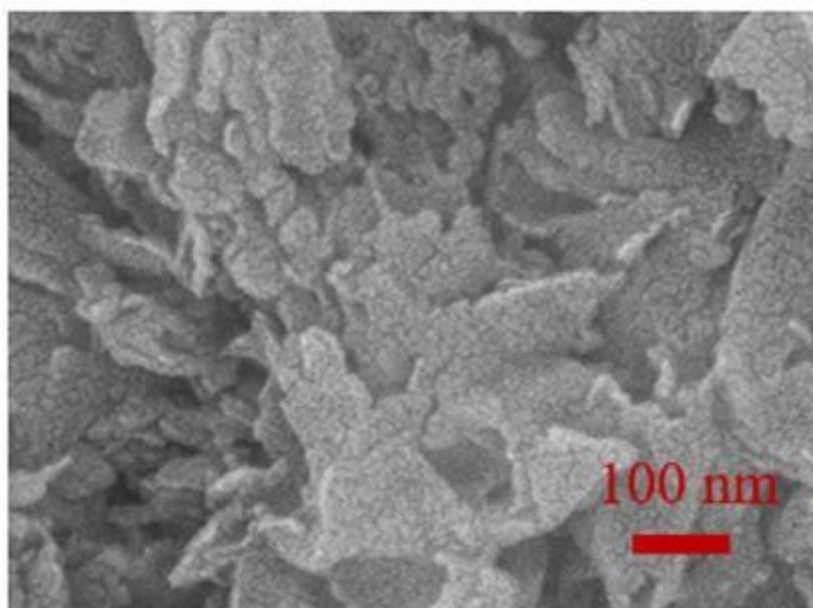


Fig.3.2 FESEM image of the graphitic carbon nitride nanofilm.

3.2.3 XRD analysis of PVDF-HFP/ g-C₃N₄ nano-composite film

The prepared nanocomposite films of PVDF-HFP/ g-C₃N₄ with varying weight percentage of g-C₃N₄ (0, 1, 3 and 5)wt% were characterised to analyse the influence of g-C₃N₄ on the structural properties of PVDF-HFP films. Fig.3.3 presents the XRD spectra of pristine PVDF-HFP (PHG0) and g-C₃N₄ incorporated PVDF-HFP films (PHG1, PHG3, PHG5). The X-ray diffraction pattern of the pristine PVDF-HFP film is similar as the reported literature. However, emergence of additional peaks in the XRD pattern of the PVDF-HFP films on incorporation of various weight percentages of g-C₃N₄ shows increment in the peaks in the XRD pattern, leading to the enhanced β - phase content. The diffraction peak at $\sim 24^\circ$, corresponding to the β - phase of the graphitic carbon nitride, exhibits a progressive increase in the intensity with rising content of graphitic carbon and shows the maximum rise at 3wt%. This enhancement in the β - phase of the thin films shows the increase in the ability of the material to introduce more dipole

interactions and modification induced by the crystalline structure of PVDF-HFP. Although at 5wt% the β - phase of the prepared film reduces in intensity, likely due to excessive filler content causing structural defects and agglomeration, which results in the phase formation hindrance. The peaks marked in the XRD spectra depicted by “*” represents g- C_3N_4 and those designated by “#” corresponds to the PVDF-HFP.

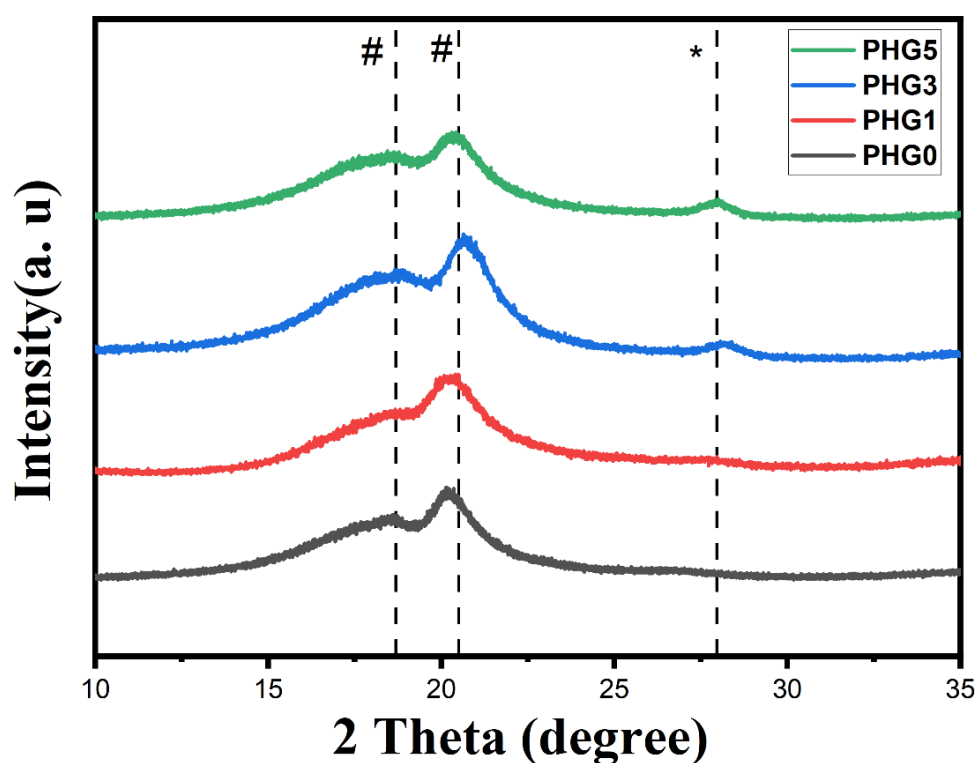


Fig. 3.3 presents the XRD spectra of pristine PVDF-HFP(PHG0) and g- C_3N_4 incorporated PVDF-HFP films (PHG1, PHG3, PHG5).

3.2.4 Thin-film FTIR analysis

The Fourier transform infrared spectroscopy of thin films of the produced flexible polymer nanocomposite is shown in Fig. 3.4. The positions of the α and β phase peaks are depicted in the picture. The β phase is important for PVDF's piezoelectric properties because of its biggest dipole moment.

The content of the β phase is calculated by the formula:

$$F(\beta) = \frac{A_{\beta}}{(K_{\alpha}) A_{\alpha} + A_{\beta}} * 100\%$$

Where $K(\beta)=7.7 \times 10^4 \text{ cm}^2/\text{mol}$ and $K(\alpha)=6.1 \times 10^4 \text{ cm}^2/\text{mol}$ are the absorption coefficients at 840 cm^{-1} and 762 cm^{-1} respectively [19]. The β phase was calculated to be 77% for bare PVDF-HFP and 89% for 3 wt% graphitic carbon nitride PVDF-HFP.

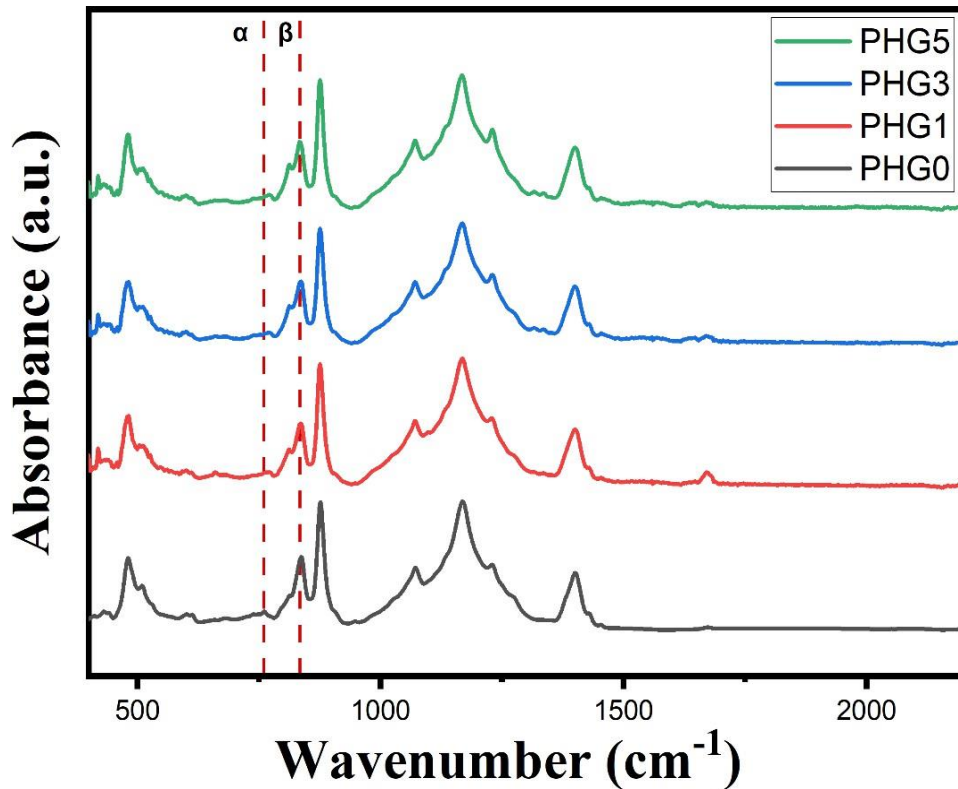


Figure 3.4. FTIR spectra of PVDF-HFP/ g-C₃N₄ thin film with different wt.% of g-C₃N₄

Wt% of g-C ₃ N ₄	β -phase
0	77
1	80
3	89
5	82

Table 2: β -Phase of g-C₃N₄ incorporated PVDF-HFP film with different wt %.

3.2.5 Polarisation-Electric field(P-E) curve

Polarisation-Electric field (P-E) plot gives the remnant polarisation of the various graphitic carbon nitride embedded PVDF-HFP nanofilms. This indicates how different dipoles align when the electric field is applied. The PVDF-HFP films' piezoelectric qualities are improved as a result of this increase in residual polarization. The given plot gives the remnant polarisation of the PVDF-HFP nanocomposite film on incorporation of the graphitic carbon nitride nanofiller. The PHG0 (0wt%) gives the remnant polarisation of the PVDF-HFP film, whereas the PMG3 gives the remnant polarisation of the PVDF-HFP with 3wt% graphitic carbon nitride which has the improved piezoelectric response of the PVDF-HFP matrix as depicted in Fig.3.5.

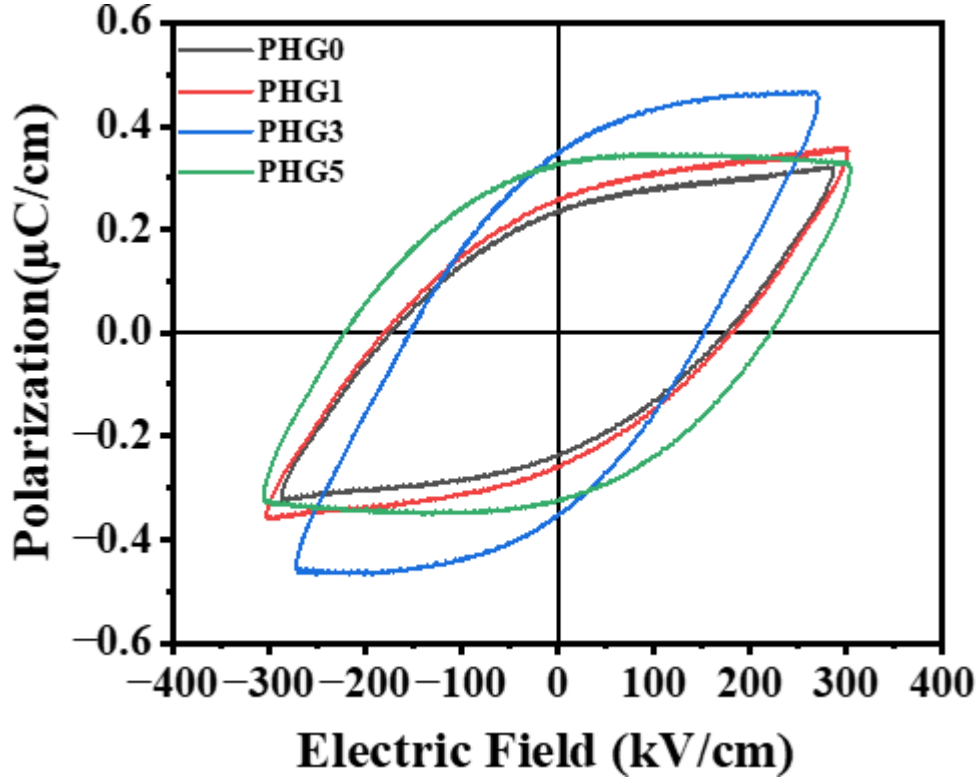


Fig.3.5 PE loop for the fabricated thin films.

3.2.6 Electrical Measurements

Graphitic carbon nitride was inserted into the manufactured PENGs with varied weight percentages (0, 1, 3, 5) to determine the piezo-responses of the corresponding PENGs with different weight percentage films. The prepared films of dimension $2\text{ cm} \times 3\text{ cm}$ were used to fabricate the PENG and the output voltages and currents were measured using an oscilloscope (Tektronix MD034) and electrometer (Keysight B2985B). As soon as pressure is applied on the PENG from both sides using the Electrodynamics shaker (Micronmev-0025), it results in the spreading of charges throughout the PENG surface after the polarisation of the dipoles and the compression and the release of force results in the generation of the alternating electrical signal resulting in the flow of charge and the generation of alternating electrical output. The application and release of force regenerates the positive and negative charges as depicted in the Fig. 3.8 . Based on different weight percentages of graphitic nanofillers in the PVDF-HFp

matrix, the PENG's open-circuit voltage and short-circuit current curves were found to be 7.2 V and 4.86 μ A, 13.2 V and 12.15 μ A, 21.2 V and 14.24 μ A, 16 V, and 13.69 μ A, respectively, for the corresponding weight percentages (0, 1, 3, 5%), as illustrated in Fig. 3.6 and Fig. 3.7.

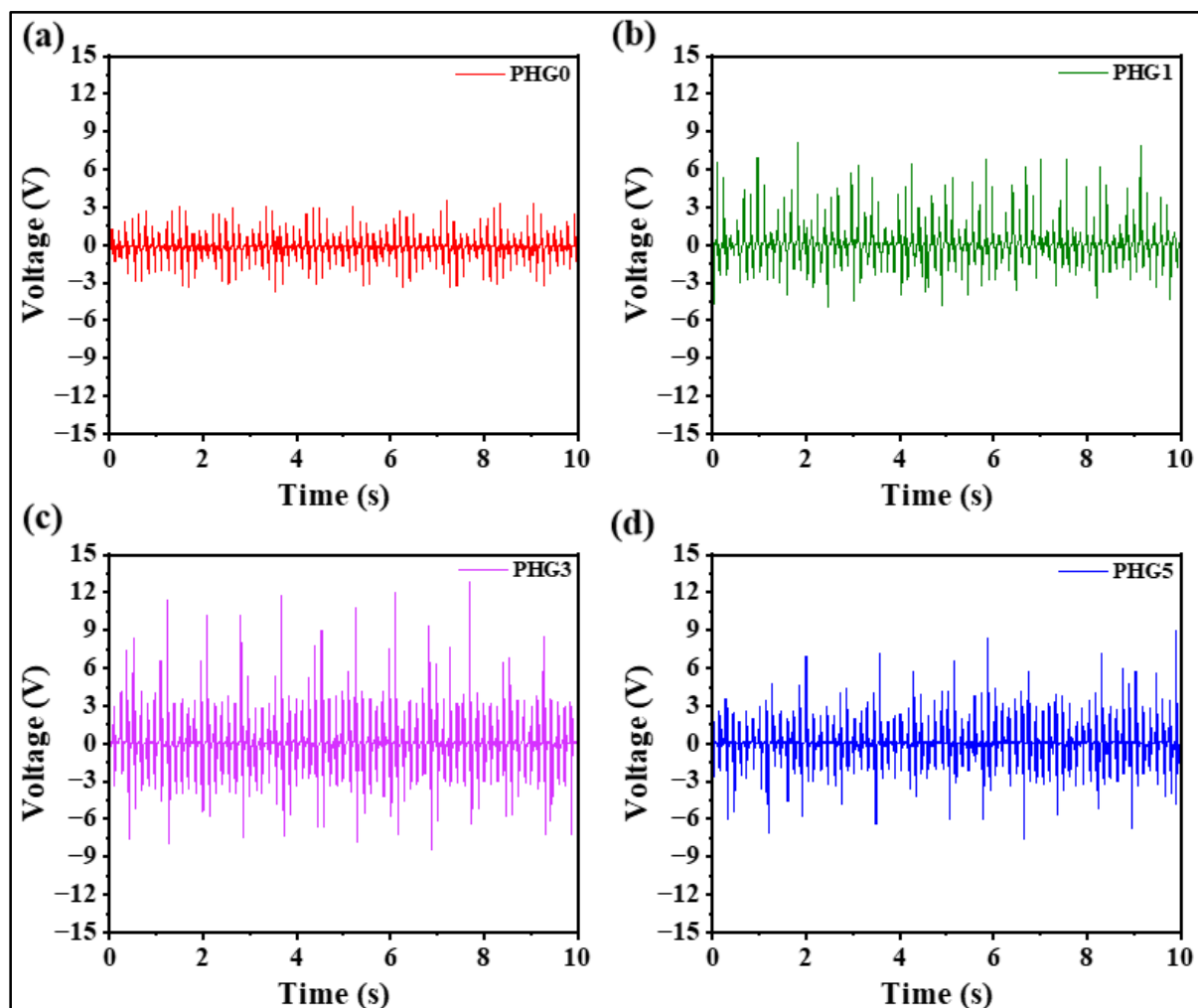


Fig. 3. 6. *PVDF-HFP open-circuit voltage (a) PVDF-HFP (b) PVDF-HFP with 1 weight percent g-C3N4 (c) PVDF-HFP with 3 weight percent g-C3N4 (d) PVDF-HFP with 5 weight percent g-C3N4.*

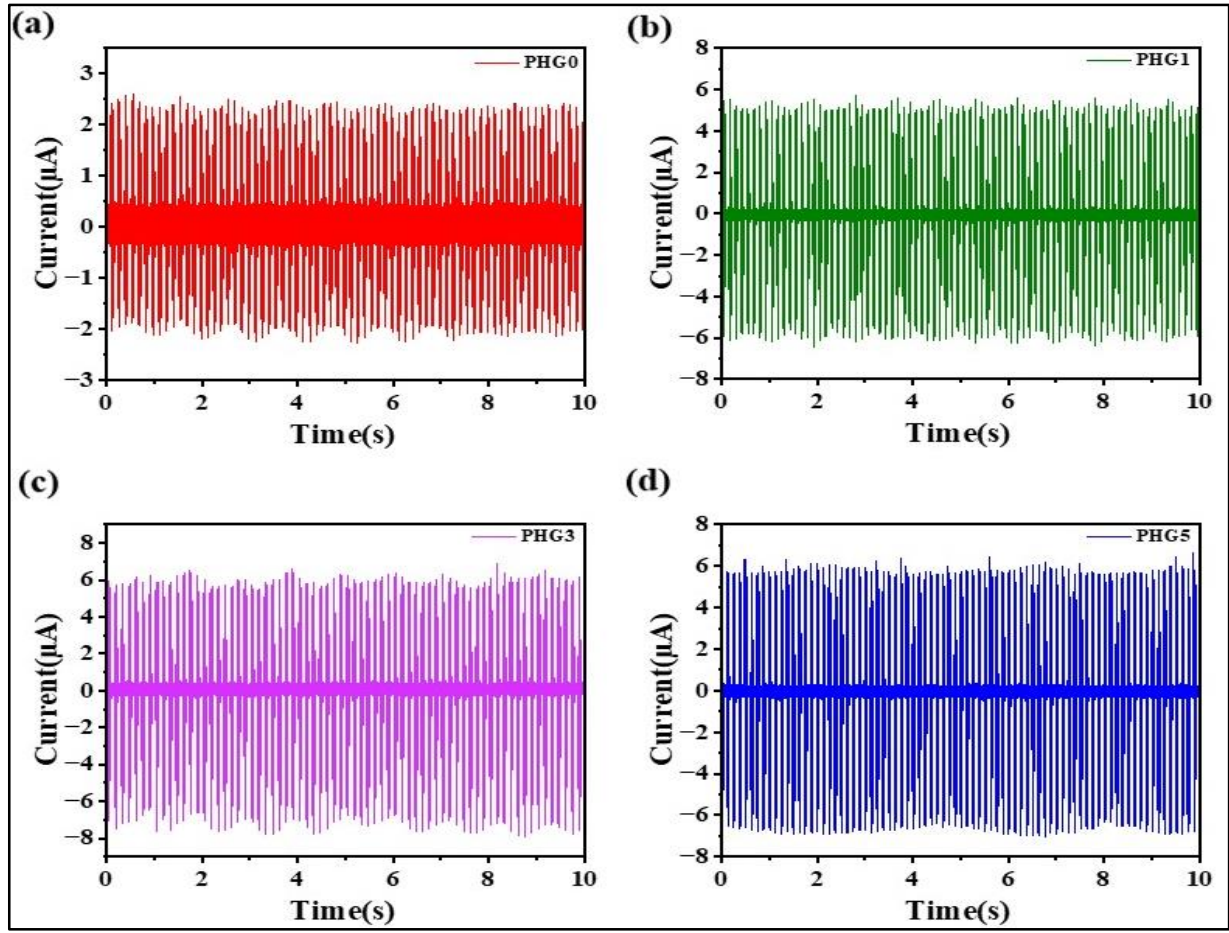


Fig.3.7 Short-circuit current for PVDF-HFP with (a) 1 weight percent g-C3N4, PVDF-HFP with another 1 weight percent g-C3N4, and PVDF-HFP with a fifth weight percent g-C3N4.

The PENG's output performance increases from 7.2V, 4.86 μ A for 0 weight percent film to 21.2V, 14.24 μ A for 3 weight percent when the nanofiller material is added to the PVDF-HFP films' matrix up to 3 weight percent. The enhanced remanent polarization of the PVDF-HFP films on incorporation of the g-C3N4 nanofillers led to the enhancement of the electrical performance of the PENG. The plot also shows the decrease in the remanent polarization of the PVDF/ g-C3N4 film at 5wt% which will eventually lead to the decrease in the voltage and current output at 5wt% to 16V and 13.69 μ A. Table 2 summarises the β -phase content, output voltage, current and remanent polarization of the fabricated PENGs devices as a function of nanofiller weight percentage.

Sample Name	β -phase (%)	Output Voltage (V)	Output current (μ A)	Remanent Polarization (μ C/cm ²)
Pure PVDF-HFP	77	7.2	4.86	0.23
PVDF-HFP/g-C ₃ N ₄ (1wt%)	83	13.2	12.15	0.25
PVDF-HFP/g-C ₃ N ₄ (3wt%)	84	21.12	14.24	0.34
PVDF-HFP/g-C ₃ N ₄ (5wt%)	80	16	13.69	0.32

Table.3 Comparison of PENG performance as a function of nanofiller concentration

As illustrated in Fig. 3.8, piezo-electrics operates on the principle of the piezoelectric effect. Initially the dipoles are arranged in a random fashion as there is no polarization of the dipoles when there is no force applied on the PENG as shown in Fig.3.8 (a). As soon as the force is applied on the device the film first starts to deform and the dipoles start to polarize inside the film and due to this polarization effect the Fig. 3.8 (b) illustrates how the electric charges are inducted on both sides of the electrode. When the charges on both electrodes build up, a voltage is produced in PENG, and the potential that is produced causes the charges to move in the external circuit. As seen in Fig. 3.8(c), the PENG device thereafter returns to its original phase when the force applied to the film is released, causing the opposite flow of charges. One cycle's completion causes the circuit to produce alternating current, and repeated cycles of this type occur multiple times during the measurement, producing a steady alternating output.

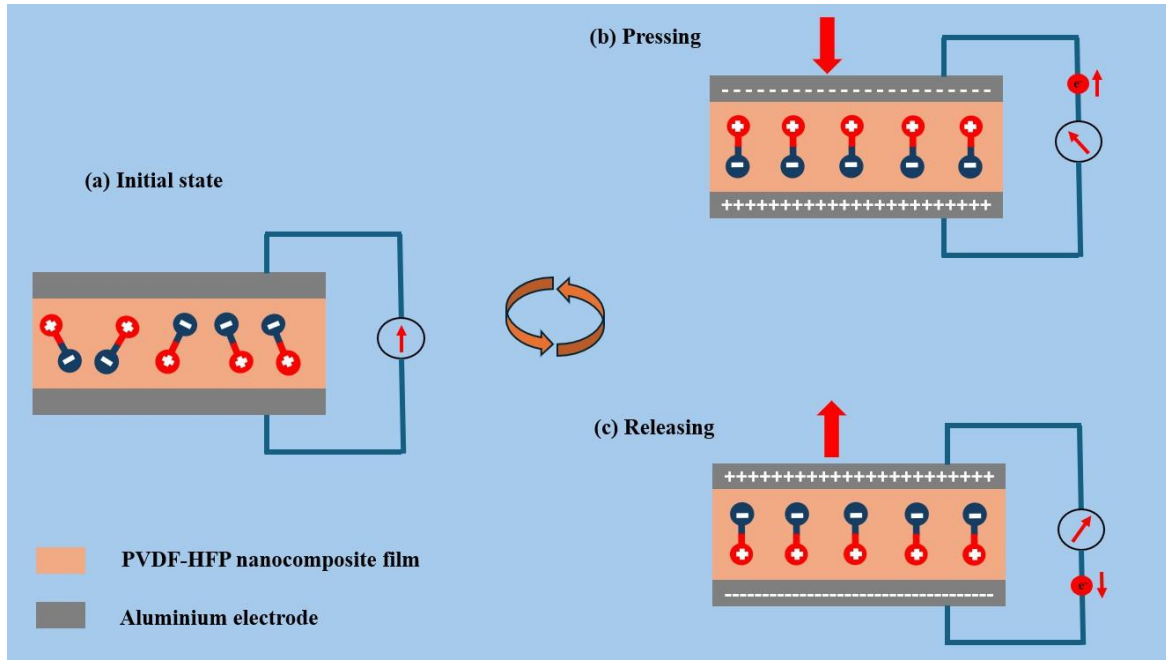


Fig. 3.8 Working Mechanism of Piezoelectric Nanogenerator

3.2.6 Application of Piezoelectric Nanogenerator

The practical application of the PENG was studied by using the thumb and the finger tapping where the PENG was put under force by thumb tapping and finger tapping which results in the output voltage of 6.36V and 2.34V, respectively which is shown in the Fig3.9 (a,b) . These results were obtained by repetitive cycles without any degradation of the films, which shows the durability of these fabricated PENG and the long life of the given output. The power generation capability of the fabricated Piezoelectric-nanogenerator was done using it to light up the LEDs. The conversion of the PENG output to direct current was done using a rectifier and then stored in a 100 μ F capacitor and the output from the charged capacitor was then used to light up the LEDs as depicted in Fig.3.9(d). The circuit diagram for the application to the light up the LED was done using the PENG is depicted in the Fig.3.9(c) .

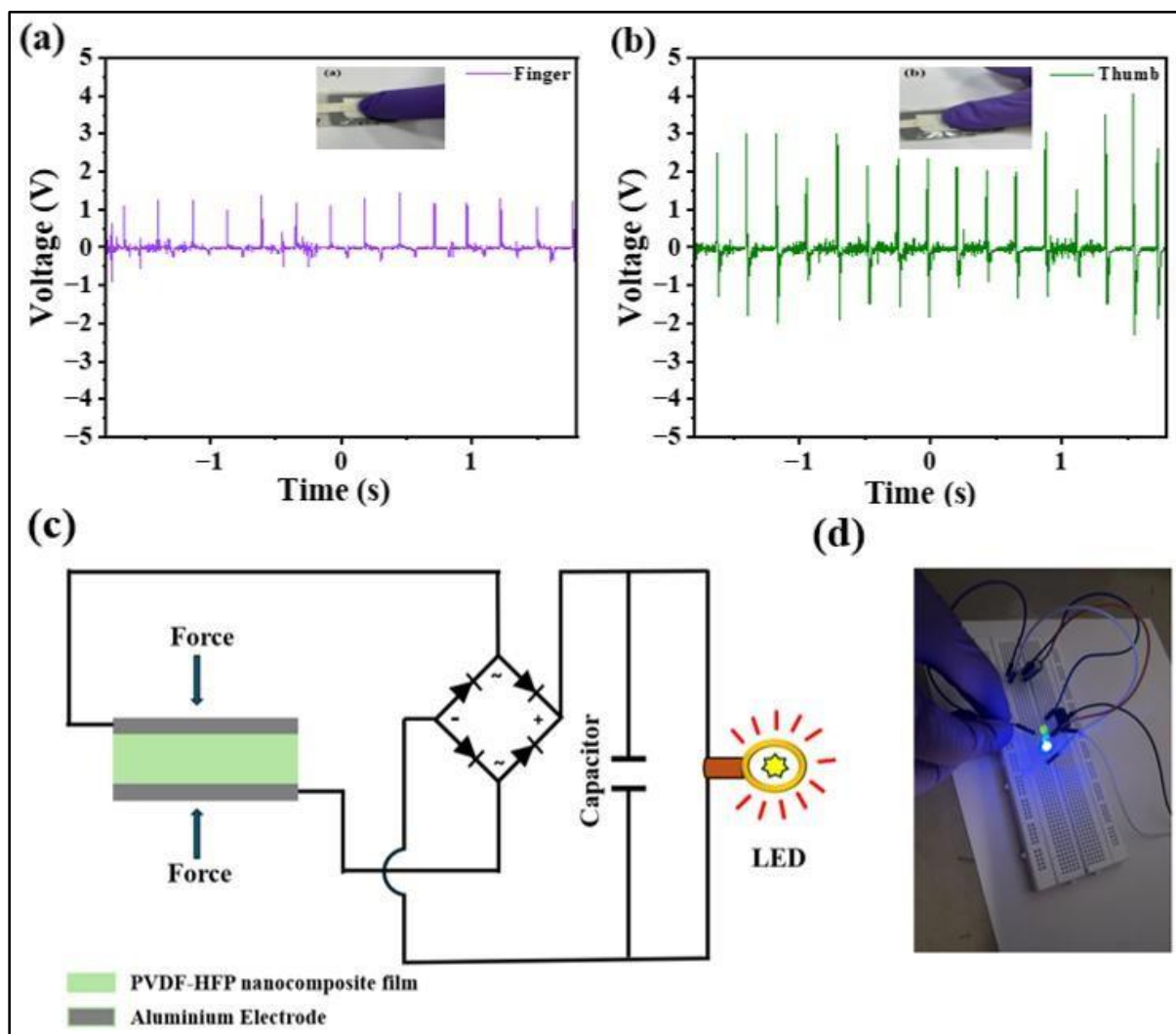


Fig. 3.9 Open-circuit voltage for PENG under the application of the force from the (a) finger (b) thumb, (c) Schematic circuit diagram for application of PENG in lighting up an LED, and (d) LED lit up by PENG

CHAPTER - 4

CONCLUSIONS AND FUTURE SCOPE

4.1 Conclusions

In this study, flexible thin films of PVDF-HFP with different weight percentages of g-C₃N₄ were synthesized successfully by drop casting method. The generation of the g-C₃N₄ powder sample is demonstrated by the XRD peak of g-C₃N₄ at 27.37°. Using field scanning electron microscopy (FESEM), the morphological analysis of the graphitic carbon nitride powder sample was conducted, verifying the successful fabrication of nanosheets. Following FTIR testing of the g-C₃N₄ doped PVDF-HFP film, PVDF-HFP's electroactive β -phase was found to have improved with the incorporation of the g-C₃N₄ powder in the film. The β -phase of the PVDF-HFP film was calculated to be 77% and that of the g-C₃N₄ doped PVDF-HFP film at 3wt% was found to be 89% which is higher than the pristine PVDF-HFP. The P-E plot for the various wt% of g-C₃N₄ in the PVDF-HFP films also shows the remanent polarization of the prepared films to be 0.23 $\mu\text{C}/\text{cm}^2$, 0.25 $\mu\text{C}/\text{cm}^2$, 0.34 $\mu\text{C}/\text{cm}^2$, 0.32 $\mu\text{C}/\text{cm}^2$ for wt.% (0, 1, 3, 5) of g-C₃N₄ respectively. These characteristics of the films corresponds to the higher efficiency of PENG. For 0%, 1%, 3%, and 5% of the total weight, the recorded output voltage and current were 7.2V and 4.86 μA , 13.2V and 12.15 μA , 21.2 V and 14.24 μA , 16 V and 13.69 μA , respectively. The 3wt% g-C₃N₄/PVDF-HFP film-based PENG exhibited the highest output performance. The improved electroactive β -phase and improved remanent polarization of the PVDF-HFP nanofilm with the addition of the graphitic carbon nitride nanofiller were the primary causes of the improved output electrical performance of the manufactured PENG. As a summary to all the above obtained results, the proposed PENG which was integrated with g-C₃N₄ showed the requisite characteristics to be used as the mechanical energy harvesting

device and power various low powered devices. This fabricated PENG is highly efficient, scalable and robust to be used as energy harvesting devices.

4.2 Future Scope

- The role of co-polymers can be further explored using graphitic carbon nitride, and the influence of thickness can also be studied.
- By using different nanomaterials such as SnSSe, graphitic carbon nitride and other TMDCs the β - phase of the nanofilms and it's copolymers can be increased leading to enhanced output.
- The use of these nanogenerators in the use of applications such as die degradation and wearable electronic devices have a very wide scope.

References

- [1] K. Ruthvik *et al.*, “High-performance triboelectric nanogenerator based on 2D graphitic carbon nitride for self-powered electronic devices,” *Mater Lett*, vol. 350, p. 134947, Nov. 2023, doi: 10.1016/J.MATLET.2023.134947.
- [2] J. Hulla, S. Sahu, A. Hayes, *Human & experimental toxicology*, 34 (2015) 1318-1321.
- [3] R.R. Chandran, B.I. Thomson, A. Natishah, J. Mary, V. Nachiyar, *Biosciences Biotechnology Research Asia*, 20 (2023) 53-68.
- [4] B. Bhushan, *Microsystem Technologies*, 21 (2015) 1137-1155.
- [5] A.V. Rane, K. Kanny, V. Abitha, S. Thomas, *Methods for synthesis of nanoparticles and fabrication of nanocomposites, Synthesis of inorganic nanomaterials*, Elsevier 2018, pp. 121-139.
- [6] S. Feng, R. Xu, *Accounts of chemical research*, 34 (2001) 239-247.
- [7] L. Chen, C.-W. Chen, C.-P. Huang, Y. Chuang, T.-B. Nguyen, C.-D. Dong, *Journal of Colloid and Interface Science*, 616 (2022) 67-80.
- [8] M. You, X. Hu, Y. Xiang, IOP Publishing, pp. 012071.
- [9] S.M. Nakhmanson, M.B. Nardelli, J. Bernholc, *Physical review letters*, 92 (2004) 115504.
- [10] B. Bera, M.D. Sarkar, *IOSR J. Appl. Phys*, 9 (2017) 95-99.
- [11] H. Pan, B. Na, R. Lv, C. Li, J. Zhu, Z. Yu, *Journal of Polymer Science Part B: Polymer Physics*, 50 (2012) 1433-1437.
- [12] V. Singh, D. Meena, H. Sharma, A. Trivedi, B. Singh, *Energy*, 239 (2022) 122125.
- [13] S.A. Han, J.H. Lee, W. Seung, J. Lee, S.W. Kim, J.H. Kim, *Small*, 17 (2021) 1903519.
- [14] S.H. Sung, N. Schnitzer, L. Brown, J. Park, R. Hovden, *Physical Review Materials*, 3 (2019) 064003.
- [15] G. Gautam, M. Kumar, B. Singh, *Materials Today: Proceedings*, 62 (2022) 3239-3243.
- [16] R.S. Sabry, A.D. Hussein, *Polymer Testing*, 79 (2019) 106001.

[17]B. P. J. C. Q. J. Z. L. W. Guang Zhu, “Triboelectric nanogenerators as a new energy technology: From fundamentals, devices, to applications,” *ELSEVIER*, 2015.

[18]K.RUTHVIK, “HIGH PERORMANCE TRIBOELECTRIC NANOGENERATOR BASED ON 2-D GRAPHITIC CARBON NITRIDE FOR SELF POWERED ELECTRONIC DEVICES,” *ELSEVIER*, 2023.

[19]B. P. J. C. Q. J. Z. L. W. Guang Zhu, “Triboelectric nanogenerators as a new energy technology: From fundamentals, devices, to applications,” *ELSEVIER*, 2015.

[20] S. Kumar, H.H. Singh, N. Khare, *Energy Conversion and Management*, 198 (2019) 111783.


APPENDIX

PLAGIARISM REPORT

1 of 55

Aditya Shivender

dissertation report shivender_Aditya.docx

 Delhi Technological University

Document Details

Submission ID

trn::27535-99827546

Submission Date

Jun 8, 2025, 11:35 AM GMT+5:30

Download Date

Jun 8, 2025, 11:41 AM GMT+5:30

File Name

dissertation report shivender_Aditya.docx


File Size

1.9 MB

50 Pages

6,779 Words

38,930 Characters

 Page 1 of 55 - Cover Page

Submission ID trn::27535-99827546

 Page 2 of 55 - Integrity Overview

Submission ID trn::27535-99827546

8% Overall Similarity

The combined total of all matches, including overlapping sources, for each database.

Filtered from the Report

- Bibliography
- Quoted Text
- Cited Text
- Small Matches (less than 8 words)

Exclusions

- 27 Excluded Matches

Match Groups

 58 Not Cited or Quoted 8%
Matches with neither in-text citation nor quotation marks

 0 Missing Quotations 0%
Matches that are still very similar to source material

 0 Missing Citation 0%
Matches that have quotation marks, but no in-text citation

 0 Cited and Quoted 0%
Matches with in-text citation present, but no quotation marks

Top Sources

4%  Internet sources

6%  Publications

4%  Submitted works (Student Papers)

Integrity Flags

1 Integrity Flag for Review

 Replaced Characters

26 suspect characters on 9 pages
Letters are swapped with similar characters from another alphabet.

Our system's algorithms look deeply at a document for any inconsistencies that would set it apart from a normal submission. If we notice something strange, we flag it for you to review.

A flag is not necessarily an indicator of a problem. However, we'd recommend you focus your attention there for further review.

Bharbi

 Page 4 of 10 | Integrity Overview

Submission ID Internal: J7YH-9BZ17546

11 - Submitted works

Vivekvaraya National Institute of Technology on 2025-05-01 +1%

12 - Publication

Derman Vatansoner Baglamci, Nammet Sait, Tahir Shah, Elias Sierra, Dombidula ... +1%

13 - Internet



Page 5 of 55

Integrity Checker

Submission ID: 661ad1_27326_286227546

23

Internet

www.mdpi.com

<1%

24

Publication

Hayden Fu, Zuchang Long, Mingxuan Lai, Junhao Cao, Rihui Zhou, Jianlang Gong, ...

<1%

25

Publication

AI REPORT

Aditya Shivender

dissertation report shivender_Aditya.docx

 Delhi Technological University

Document Details

Submission ID

trn:oid::27535:99827546

Submission Date

Jun 8, 2025, 11:35 AM GMT+5:30

Download Date

Jun 8, 2025, 11:41 AM GMT+5:30

File Name

dissertation report shivender_Aditya.docx

File Size

1.9 MB

50 Pages

6,779 Words

38,930 Characters



Page 1 of 52 • Cover Page

Submission ID trn:oid::27535:99827546



Page 2 of 52 • AI Writing Overview

Submission ID trn:oid::27535:99827546

*% detected as AI

AI detection includes the possibility of false positives. Although some text in this submission is likely AI generated, scores below the 20% threshold are not surfaced because they have a higher likelihood of false positives.

Caution: Review required.

It is essential to understand the limitations of AI detection before making decisions about a student's work. We encourage you to learn more about Turnitin's AI detection capabilities before using the tool.

Disclaimer

Our AI writing assessment is designed to help educators identify text that might be prepared by a generative AI tool. Our AI writing assessment may not always be accurate (it may misidentify writing that is likely AI generated as AI generated and AI paraphrased or likely AI generated and AI paraphrased writing as only AI generated) so it should not be used as the sole basis for adverse actions against a student. It takes further scrutiny and human judgment in conjunction with an organization's application of its specific academic policies to determine whether any academic misconduct has occurred.

Frequently Asked Questions

How should I interpret Turnitin's AI writing percentage and false positives?

The percentage shown in the AI writing report is the amount of qualifying text within the submission that Turnitin's AI writing detection model determines was either likely AI-generated text from a large-language model or likely AI-generated text that was likely revised using an AI-paraphrase tool or word spinner.

False positives (incorrectly flagging human-written text as AI-generated) are a possibility in AI models.

AI detection scores under 20%, which we do not surface in new reports, have a higher likelihood of false positives. To reduce the likelihood of misinterpretation, no score or highlights are attributed and are indicated with an asterisk in the report (*%).

The AI writing percentage should not be the sole basis to determine whether misconduct has occurred. The reviewer/instructor should use the percentage as a means to start a formative conversation with their student and/or use it to examine the submitted assignment in accordance with their school's policies.

What does 'qualifying text' mean?

Our model only processes qualifying text in the form of long-form writing. Long-form writing means individual sentences contained in paragraphs that make up a longer piece of written work, such as an essay, a dissertation, or an article, etc. Qualifying text that has been determined to be likely AI-generated will be highlighted in cyan in the submission, and likely AI-generated and then likely AI-paraphrased will be highlighted purple.

Non-qualifying text, such as bullet points, numbered lists, tables, etc., will not be assessed and can exist anywhere between the qualifying highlights and the



CERTIFICATES OF PARTICIPATION



PROOF OF REGISTRATION

----- Forwarded message -----

From: <ann@rajdhani.du.ac.in>

Date: Tue, 25 Mar, 2025, 21:17

Subject: E-Certificate for Presenting Paper in
ICANN-2025

To: <adityaanand14112001@gmail.com>

Dear ADITYA ANAND,

We hope this email finds you well.

We are delighted to share your e-certificate for presenting Graphitic-carbon nitride embedded PVDF-HFP nanocomposite film for improved performance of piezoelectric nanogenerator in International Conference on "Advances in Nanomaterials and Nanotechnology", held from 05-06 March 2025 at Rajdhani College, University of Delhi.

Thank you for your valuable contributions and active participation in the conferece. We believe your insights and discussions have enriched the learning experience for all participants.

With warm regards,

Dr. Jasvir
Convenor
Rajdhani College, University of Delhi

PROOF OF ACCEPTANCE

----- Forwarded message -----

From: <ann@rajdhani.du.ac.in>

Date: Tue, 25 Mar, 2025, 21:17

Subject: E-Certificate for Presenting Paper in
ICANN-2025

To: <adityaanand14112001@gmail.com>

Dear ADITYA ANAND,

We hope this email finds you well.

We are delighted to share your e-certificate for presenting Graphitic-carbon nitride embedded PVDF-HFP nanocomposite film for improved performance of piezoelectric nanogenerator in International Conference on "Advances in Nanomaterials and Nanotechnology", held from 05-06 March 2025 at Rajdhani College, University of Delhi.

Thank you for your valuable contributions and active participation in the conferece. We believe your insights and discussions have enriched the learning experience for all participants.

With warm regards,

Dr. Jasvir

Convenor

Rajdhani College, University of Delhi

SUBMITTED MANUSCRIPT

Discover Materials - Receipt of
Manuscript 'Graphitic-Carbon
Nitride Embedded...' Inbox



Discover Materials 26 May
to me ▾



Ref: Submission ID d365970f-10bd-494d-b3c5-a009143c9636

Dear Dr Bhandari,

Please note that you are listed as a co-author on the manuscript "Graphitic-Carbon Nitride Embedded PVDF-HFP Nanocomposite Film for Improved Performance of Piezoelectric Nanogenerator", which was submitted to Discover Materials on 26 May 2025 UTC.

If you have any queries related to this manuscript please contact the corresponding author, who is solely responsible for communicating with the journal.

Kind regards,

Assistant Editors

...

SUBMITTED PAPER

Graphitic-Carbon Nitride Embedded PVDF-HFP Nanocomposite Film for Improved Performance of Piezoelectric Nanogenerator

Shivender Singh Bhandari^a, Aditya Anand^a, Shilpa Rana^a, Dibyajyoti Giri^a, Jasvir Dalal ^{b,1},
Bharti Singh ^{a,*}

^a *Department of Applied Physics, Delhi Technological University, Main Bawana Road, Delhi, 110042, India*

^b *Department of Physics, Rajdhani College, Delhi University, Delhi-110015, India*

Abstract

Piezoelectric nanogenerators (PENGs) are emerging as potential energy sources for powering wearable electronic devices and IoT applications by harvesting mechanical energy from the environment. In this study, a flexible PENG was fabricated using PVDF-HFP polymer films embedded with different weight percentages (0, 1, 3, and 5 wt%) of graphitic carbon nitride (g-C₃N₄) nanofillers. The structural and morphological properties of the fabricated films were characterized by X-ray diffraction (XRD), Fourier-transform infrared spectroscopy (FTIR), and scanning electron microscopy (SEM), confirming the successful incorporation of g-C₃N₄. The nanocomposite films were assembled into PENG devices and their output performance was evaluated through application of the electrodynamic shaker. The results show a considerable enhancement in open-circuit voltage of 21.2 V and short-circuit current of 14.24 μ A with increasing g-C₃N₄ content, compared to pure PVDF-HFP films. The improved performance is attributed to the influence of g-C₃N₄ nanofillers in promoting the electroactive phase in the polymer matrix. This work highlights the potential of g-C₃N₄-based PVDF-HFP nanocomposite films for developing efficient, flexible, and sustainable energy harvesting devices for self-powered wearable electronics.

¹ Corresponding Authors Email: jasvirdalal2012@gmail.com (J. Dalal), and bhartisingh@dtu.ac.in (B. Singh)